



NOAA Technical Memorandum NWS WR-221

**UTILIZATION OF THE BULK RICHARDSON NUMBER,
HELICITY AND SOUNDING MODIFICATION IN THE
ASSESSMENT OF THE SEVERE CONVECTIVE
STORMS OF 3 AUGUST 1992**

**Eric C. Evenson
Weather Service Forecast Office
Great Falls, Montana**

November 1993

**U.S. DEPARTMENT OF
COMMERCE**

/ National Oceanic and
Atmospheric Administration

/ National Weather
Service



NOAA TECHNICAL MEMORANDA
National Weather Service, Western Region Subseries

The National Weather Service (NWS) Western Region (WR) Subseries provides an informal medium for the documentation and quick dissemination of results not appropriate, or not yet ready, for formal publication. The series is used to report on work in progress, to describe technical procedures and practices, or to relate progress to a limited audience. These Technical Memoranda will report on investigations devoted primarily to regional and local problems of interest mainly to personnel, and hence will not be widely distributed.

Papers 1 to 25 are in the former series, ESSA Technical Memoranda, Western Region Technical Memoranda (WRTM); papers 24 to 59 are in the former series, ESSA Technical Memoranda, Weather Bureau Technical Memoranda (WBTM). Beginning with 60, the papers are part of the series, NOAA Technical Memoranda NWS. Out-of-print memoranda are not listed.

Papers 2 to 22, except for 5 (revised edition), are available from the National Weather Service Western Region, Scientific Services Division, P.O. Box 11188, Federal Building, 125 South State Street, Salt Lake City, Utah 84147. Paper 5 (revised edition), and all others beginning with 25 are available from the National Technical Information Service, U.S. Department of Commerce, Sills Building, 5285 Port Royal Road, Springfield, Virginia 22161. Prices vary for all paper copies; microfiche are \$3.60. Order by accession number shown in parentheses at end of each entry.

ESSA Technical Memoranda (WRTM)

- 2 Climatological Precipitation Probabilities. Compiled by Lucianne Miller, December 1965.
- 3 Western Region Pre- and Post-FP-3 Program, December 1, 1965, to February 20, 1966. Edward D. Diemer, March 1966.
- 5 Station Descriptions of Local Effects on Synoptic Weather Patterns. Philip Williams, Jr., April 1966 (Revised November 1967, October 1969). (PB-17800)
- 8 Interpreting the RAREP. Herbert P. Benner, May 1966 (Revised January 1967).
- 11 Some Electrical Processes in the Atmosphere. J. Latham, June 1966.
- 17 A Digitalized Summary of Radar Echoes within 100 Miles of Sacramento, California. J. A. Youngberg and L. B. Overas, December 1966.
- 21 An Objective Aid for Forecasting the End of East Winds in the Columbia Gorge, July through October. D. John Coparanis, April 1967.
- 22 Derivation of Radar Horizons in Mountainous Terrain. Roger G. Pappas, April 1967.

ESSA Technical Memoranda, Weather Bureau Technical Memoranda (WBTM)

- 25 Verification of Operation Probability of Precipitation Forecasts, April 1966-March 1967. W. W. Dickey, October 1967. (PB-176240)
- 26 A Study of Winds in the Lake Mead Recreation Area. R. P. Augulis, January 1968. (PB-177830)
- 28 Weather Extremes. R. J. Schmidli, April 1968 (Revised March 1986). (PB86 177672/AS). (Revised October 1991 - PB92-115062/AS)
- 29 Small-Scale Analysis and Prediction. Philip Williams, Jr., May 1968. (PB178425)
- 30 Numerical Weather Prediction and Synoptic Meteorology. CPT Thomas D. Murphy, USAF, May 1968. (AD 673365)
- 31 Precipitation Detection Probabilities by Salt Lake ARTC Radars. Robert K. Belesky, July 1968. (PB 179084)
- 32 Probability Forecasting—A Problem Analysis with Reference to the Portland Fire Weather District. Harold S. Ayer, July 1968. (PB 179289)
- 36 Temperature Trends in Sacramento—Another Heat Island. Anthony D. Lentini, February 1969. (PB 183055)
- 37 Disposal of Logging Residues Without Damage to Air Quality. Owen P. Cramer, March 1969. (PB 183057)
- 39 Upper-Air Lows Over Northwestern United States. A.L. Jacobson, April 1969. PB 184296)
- 40 The Man-Machine Mix in Applied Weather Forecasting in the 1970s. L.W. Snellman, August 1969. (PB 185068)
- 43 Forecasting Maximum Temperatures at Helena, Montana. David E. Olsen, October 1969. (PB 185785)
- 44 Estimated Return Periods for Short-Duration Precipitation in Arizona. Paul C. Kangieser, October 1969. (PB 187763)
- 46 Applications of the Net Radiometer to Short-Range Fog and Stratus Forecasting at Eugene, Oregon. L. Yee and E. Bates, December 1969. (PB 190476)
- 47 Statistical Analysis as a Flood Routing Tool. Robert J.C. Burnash, December 1969. (PB 188744)
- 48 Tsunami. Richard P. Augulis, February 1970. (PB 190157)
- 49 Predicting Precipitation Type. Robert J.C. Burnash and Floyd E. Hug, March 1970. (PB 190962)
- 50 Statistical Report on Aeroallergens (Pollens and Molds) Fort Huachuca, Arizona, 1969. Wayne S. Johnson, April 1970. (PB 191743)
- 51 Western Region Sea State and Surf Forecaster's Manual. Gordon C. Shields and Gerald B. Burdwell, July 1970. (PB 193102)
- 52 Sacramento Weather Radar Climatology. R.G. Pappas and C. M. Veliquette, July 1970. (PB 193347)
- 54 A Refinement of the Vorticity Field to Delineate Areas of Significant Precipitation. Barry B. Aronovitch, August 1970.
- 55 Application of the SSARR Model to a Basin without Discharge Record. Vail Schermerhorn and Donal W. Kuehl, August 1970. (PB 194394)
- 56 Areal Coverage of Precipitation in Northwestern Utah. Philip Williams, Jr., and Werner J. Heck, September 1970. (PB 194389)
- 57 Preliminary Report on Agricultural Field Burning vs. Atmospheric Visibility in the Willamette Valley of Oregon. Earl M. Bates and David O. Chilcote, September 1970. (PB 194710)
- 58 Air Pollution by Jet Aircraft at Seattle-Tacoma Airport. Wallace R. Donaldson, October 1970. (COM 71 00017)
- 59 Application of PE Model Forecast Parameters to Local-Area Forecasting. Leonard W. Snellman, October 1970. (COM 71 00016)
- 60 An Aid for Forecasting the Minimum Temperature at Medford, Oregon, Arthur W. Fritz, October 1970. (COM 71 00120)
- 63 700-mb Warm Air Advection as a Forecasting Tool for Montana and Northern Idaho. Norris E. Woerner, February 1971. (COM 71 00349)
- 64 Wind and Weather Regimes at Great Falls, Montana. Warren B. Price, March 1971.
- 65 Climate of Sacramento, California. Tony Martini, April 1990. (Fifth Revision) (PB89 207781/AS)
- 66 A Preliminary Report on Correlation of ARTCC Radar Echoes and Precipitation. Wilbur K. Hall, June 1971. (COM 71 00829)
- 69 National Weather Service Support to Soaring Activities. Ellis Burton, August 1971. (COM 71 00958)
- 71 Western Region Synoptic Analysis-Problems and Methods. Philip Williams, Jr., February 1972. (COM 72 10433)
- 74 Thunderstorms and Hail Days Probabilities in Nevada. Clarence M. Sakamoto, April 1972. (COM 72 10554)
- 75 A Study of the Low Level Jet Stream of the San Joaquin Valley. Ronald A. Willis and Philip Williams, Jr., May 1972. (COM 72 10707)
- 76 Monthly Climatological Charts of the Behavior of Fog and Low Stratus at Los Angeles International Airport. Donald M. Gales, July 1972. (COM 72 11140)
- 77 A Study of Radar Echo Distribution in Arizona During July and August. John E. Hales, Jr. July 1972. (COM 72 11136)
- 78 Forecasting Precipitation at Bakersfield, California, Using Pressure Gradient Vectors. Earl T. Riddiough, July 1972. (COM 72 11146)
- 79 Climate of Stockton, California. Robert C. Nelson, July 1972. (COM 72 10920)
- 80 Estimation of Number of Days Above or Below Selected Temperatures. Clarence M. Sakamoto, October 1972. (COM 72 10021)
- 81 An Aid for Forecasting Summer Maximum Temperatures at Seattle, Washington. Edgar G. Johnson, November 1972. (COM 73 10150)
- 82 Flash Flood Forecasting and Warning Program in the Western Region. Philip Williams, Jr., Chester L. Glenn, and Roland L. Raetz, December 1972, (Revised March 1978). (COM 73 10251)
- 83 A comparison of Manual and Semiautomatic Methods of Digitizing Analog Wind Records. Glenn E. Rasch, March 1973. (COM 73 10669)
- 86 Conditional Probabilities for Sequences of Wet Days at Phoenix, Arizona. Paul C. Kangieser, June 1973. (COM 73 11264)
- 87 A Refinement of the Use of K-Values in Forecasting Thunderstorms in Washington and Oregon. Robert Y.G. Lee, June 1973. (COM 73 11276)
- 89 Objective Forecast Precipitation Over the Western Region of the United States. Julia N. Paegle and Larry P. Kierulff, September 1973. (COM 73 11946/3AS)
- 91 Arizona "Eddy" Tornadoes. Robert S. Ingram, October 1973. (COM 73 10465)
- 92 Smoke Management in the Willamette Valley. Earl M. Bates, May 1974. (COM 74 10271/AS)
- 93 An Operational Evaluation of 500-mb Type Regression Equations. Alexander E. MacDonald, June 1974. (COM 74 11407/AS)
- 94 Conditional Probability of Visibility Less than One-Half Mile in Radiation Fog at Fresno, California. John D. Thomas, August 1974. (COM 74 11555/AS)
- 95 Climate of Flagstaff, Arizona. Paul W. Sorenson, and updated by Reginald W. Preston, January 1987. (PB87 143160/AS)
- 96 Map type Precipitation Probabilities for the Western Region. Glenn E. Rasch and Alexander E. MacDonald, February 1975. (COM 75 10428/AS)
- 97 Eastern Pacific Cut-Off Low of April 21-28, 1974. William J. Alder and George R. Miller, January 1976. (PB 250 711/AS)
- 98 Study on a Significant Precipitation Episode in Western United States. Ira S. Brenner, April 1976. (COM 75 10719/AS)
- 99 A Study of Flash Flood Susceptibility-A Basin in Southern Arizona. Gerald Williams, August 1975. (COM 75 11360/AS)
- 102 A Set of Rules for Forecasting Temperatures in Napa and Sonoma Counties. Wesley L. Tuft, October 1975. (PB 246 902/AS)
- 103 Application of the National Weather Service Flash-Flood Program in the Western Region. Gerald Williams, January 1976. (PB 253 053/AS)
- 104 Objective Aids for Forecasting Minimum Temperatures at Reno, Nevada, During the Summer Months. Christopher D. Hill, January 1976. (PB 252 866/AS)
- 105 Forecasting the Mono Wind. Charles P. Ruscha, Jr., February 1976. (PB 254 650)
- 106 Use of MOS Forecast Parameters in Temperature Forecasting. John C. Plankinton, Jr., March 1976. (PB 254 649)
- 107 Map Types as Aids in Using MOS PoPs in Western United States. Ira S. Brenner, August 1976. (PB 259 594)
- 108 Other Kinds of Wind Shear. Christopher D. Hill, August 1976. (PB 260 437/AS)
- 109 Forecasting North Winds in the Upper Sacramento Valley and Adjoining Forests. Christopher E. Fontana, September 1976. (PB 273 677/AS)
- 110 Cool Inflow as a Weakening Influence on Eastern Pacific Tropical Cyclones. William J. Denney, November 1976. (PB 264 655/AS)
- 112 The MAN/MOS Program. Alexander E. MacDonald, February 1977. (PB 265 941/AS)
- 113 Winter Season Minimum Temperature Formula for Bakersfield, California, Using Multiple Regression. Michael J. Oard, February 1977. (PB 273 694/AS)
- 114 Tropical Cyclone Kathleen. James R. Fors, February 1977. (PB 273 676/AS)
- 116 A Study of Wind Gusts on Lake Mead. Bradley Colman, April 1977. (PB 268 847)
- 117 The Relative Frequency of Cumulonimbus Clouds at the Nevada Test Site as a Function of K-Value. R.F. Quiring, April 1977. (PB 272 831)
- 118 Moisture Distribution Modification by Upward Vertical Motion. Ira S. Brenner, April 1977. (PB 268 740)
- 119 Relative Frequency of Occurrence of Warm Season Echo Activity as a Function of Stability Indices Computed from the Yucca Flat, Nevada, Rawinsonde. Darryl Randerson, June 1977. (PB 271 290/AS)
- 121 Climatological Prediction of Cumulonimbus Clouds in the Vicinity of the Yucca Flat Weather Station. R.F. Quiring, June 1977. (PB 271 704/AS)
- 122 A Method for Transforming Temperature Distribution to Normality. Morris S. Webb, Jr., June 1977. (PB 271 742/AS)
- 124 Statistical Guidance for Prediction of Eastern North Pacific Tropical Cyclone Motion - Part I. Charles J. Neumann and Preston W. Leftwich, August 1977. (PB 272 651)
- 125 Statistical Guidance on the Prediction of Eastern North Pacific Tropical Cyclone Motion - Part II. Preston W. Leftwich and Charles J. Neumann, August 1977. (PB 273 155/AS)
- 126 Climate of San Francisco. E. Jan Null, February 1978. Revised by George T. Perich, April 1988. (PB88 208624/AS)
- 127 Development of a Probability Equation for Winter-Type Precipitation Patterns in Great Falls, Montana. Kenneth B. Mielke, February 1978. (PB 281 387/AS)
- 128 Hand Calculator Program to Compute Parcel Thermal Dynamics. Dan Gudge, April 1978. (PB 283 080/AS)
- 129 Fire whirls. David W. Goens, May 1978. (PB 283 866/AS)
- 130 Flash-Flood Procedure. Ralph C. Hatch and Gerald Williams, May 1978. (PB 286 014/AS)
- 131 Automated Fire-Weather Forecasts. Mark A. Molner and David E. Olsen, September 1978. (PB 289 916/AS)
- 132 Estimates of the Effects of Terrain Blocking on the Los Angeles WSR-74C Weather Radar. R.G. Pappas, R.Y. Lee, B.W. Finke, October 1978. (PB 289767/AS)
- 133 Spectral Techniques in Ocean Wave Forecasting. John A. Jannuzzi, October 1978. (PB291317/AS)
- 134 Solar Radiation. John A. Jannuzzi, November 1978. (PB291195/AS)
- 135 Application of a Spectrum Analyzer in Forecasting Ocean Swell in Southern California Coastal Waters. Lawrence P. Kierulff, January 1979. (PB292716/AS)
- 136 Basic Hydrologic Principles. Thomas L. Dietrich, January 1979. (PB292247/AS)
- 137 LFM 24-Hour Prediction of Eastern Pacific Cyclones Refined by Satellite Images. John R. Zimmerman and Charles P. Ruscha, Jr., January 1979. (PB294324/AS)
- 138 A Simple Analysis/Diagnosis System for Real Time Evaluation of Vertical Motion. Scott Helfick and James R. Fors, February 1979. (PB294216/AS)
- 139 Aids for Forecasting Minimum Temperature in the Wenatchee Frost District. Robert S. Robinson, April 1979. (PB298339/AS)
- 140 Influence of Cloudiness on Summertime Temperatures in the Eastern Washington Fire Weather district. James Holcomb, April 1979. (PB298674/AS)
- 141 Comparison of LFM and MFM Precipitation Guidance for Nevada During Doreen. Christopher Hill, April 1979. (PB298613/AS)

NOAA Technical Memorandum NWS WR-221

**UTILIZATION OF THE BULK RICHARDSON NUMBER,
HELICITY AND SOUNDING MODIFICATION IN THE
ASSESSMENT OF THE SEVERE CONVECTIVE
STORMS OF 3 AUGUST 1992**

**Eric C. Evenson
Weather Service Forecast Office
Great Falls, Montana**

November 1993

*UNITED STATES
DEPARTMENT OF COMMERCE
Ronald H. Brown, Secretary*

*National Oceanic and
Atmospheric Administration
(Vacant), Under Secretary
and Administrator*

*National Weather Service
Elbert W. Friday, Jr., Assistant
Administrator for Weather Services*



This publication has been reviewed
and is approved for publication by
Scientific Services Division,
Western Region

A handwritten signature in black ink, appearing to read "Ken Mielke". The signature is written in a cursive, flowing style.

Kenneth B. Mielke, Chief
Scientific Services Division
Salt Lake City, Utah

TABLE OF CONTENTS

I.	INTRODUCTION	1
II.	COMPOSITE ANALYSIS	1
III.	SURFACE ANALYSIS	2
IV.	THETA-E ANALYSES	3
V.	SOUNDING AND HODOGRAPH DATA	3
VI.	BULK RICHARDSON NUMBER	3
VII.	HELICITY	5
VIII.	CONCLUSIONS	5
IX.	ACKNOWLEDGEMENTS	6
X.	REFERENCES	6

TABLE OF FIGURES

- Figure 1: Lot of known severe weather events across Hill county in north-central Montana on 3 August 1992. (Reports from Storm Data and local storm reports.) T = tornado W = wind damage A = hail greater than 3/4 inch diameter. 8
- Figure 2: Composite analysis at 1200 UTC on 3 August 1992. Arrow represent jet maxima at various levels. Dotted line represents the 850 mb thermal ridge. Large dashed line denotes 700 mb short-wave trough. Triangular line indicates thermal trough at 500 mb. Jagged dot-dashed line represents diffluence at the 500 mb level. Thin dashed lines represent surface isodrosotherms analyzed every 5°F (>50°F). Stippled area denotes Lifted Indices less than or equal to zero. 9
- Figure 3: Same as Figure 2 except at 0000 UTC on 4 August 1992.10
- Figure 4: 1800 UTC surface analysis on 3 August 1992. Solid lines represent isodrosotherms analyzed every 5°F.11
- Figure 5: 0000 UTC surface analysis on 4 August 1992. Solid lines represent isodrosotherms analyzed every 5°F.12
- Figure 6: 1200 UTC 700 mb equivalent potential temperature analysis on 3 August 1992. Solid lines represent equivalent isentropes analyzed every 5K.13

Figure 7:	0000 UTC 700 mb equivalent potential temperature analysis on 4 August 1992. Solid lines represent equivalent isentropes analyzed every 5K.14
Figure 8:	1200 UTC Great Falls, Montana (GTF) SkewT-logP sounding on 3 August 1992.15
Figure 9:	1200 UTC Great Falls, Montana (GTF) hodograph on 3 August 1992 in ms^{-1} . Points along the hodograph indicate thousands of feet above mean sea-level.16
Figure 10:	Same as Figure 8 except at 0000 UTC on 4 August 1992.17
Figure 11:	Same as Figure 9 except at 0000 UTC on 4 August 1992.18
Figure 12:	0000 UTC 4 August 1992 modified SkewT-logP sounding for Havre, Montana (HVR) via the SHARP Workstation.19
Figure 13:	0000 UTC 4 August 1992 modified hodograph for Havre, Montana (HVR) via the SHARP Workstation using the default storm motion (70% of the magnitude and 30° to the right of the 0-6 km mean wind).20
Figure 14:	0000 UTC 4 August 1992 modified Havre, Montana (HVR) hodograph using the observed storm motion from radar data.21

Utilization of the Bulk Richardson Number, Helicity and Sounding Modification in the Assessment of the Severe Convective Storms of 3 August 1992

Eric C. Evenson
WSFO Great Falls

I. INTRODUCTION

On August 3, 1992, a severe thunderstorm developed during the early evening hours over north-central Montana (Fig. 1). The severe thunderstorm dropped baseball-size hail, causing extensive damage to homes, vehicles, and crops. An F0 tornado and one report of wind damage was also reported.

When assessing the threat of severe weather, forecasters typically ask the question, "What type of storm structure can be expected"? One way to forecast storm type is through the use of the Bulk Richardson Number (BRN) as defined by Weisman and Klemp (1982, 1984). The BRN involves a relationship between storm type, wind shear, and buoyancy and is especially useful in determining isolated supercell development. This study examines the conditions that led to the initiation of the severe convection, forecasting the location of severe weather, and assessing the type of storm structure using the BRN. The role of helicity and sounding modification is also examined.

II. COMPOSITE ANALYSIS

Johns and Doswell (1992) note that composite analyses, prepared daily by the forecasters at the SEvere Local Storms (SELS) unit of the National Severe

Storms Forecast Center (NSSFC), are a useful technique in observing those meteorological parameters necessary for the development of severe local storms. From the composite chart, wind, moisture, and temperature patterns at various levels in the atmosphere can be visualized. Also, these patterns can be compared to the orientation of the static stability fields at a given time. The SELS forecaster uses the chart to help define and delineate areas in which severe thunderstorm development is most likely.

The composite analysis (Fig. 2) valid at 1200 UTC on 3 August showed several features conducive to the generation of severe thunderstorms. A north-south oriented stationary surface front extended from east of Cut Bank, Montana (CTB), through Great Falls (GTF) and southeast through Billings (BIL). Surface dew points were 50° F or greater over much of Montana east of the Continental Divide. At 850 mb, southeasterly low-level winds of 25 knots prevailed across eastern Montana. Also at the 850 mb level, a thermal ridge extended from southern Alberta through western Montana and continued south into western Utah. Progressing upward to the 700 mb level, a positively tilted short-wave trough was located across southern Alberta and into the northeast portion of Washington state. At 500 mb, a low pressure trough and associated cold pool of air was situated over southeast British Columbia. Across eastern Washington

state, northern Idaho, and western Montana, a mid-level wind maximum (500 mb) of 35 knots was observed. Difffluence was also noted at 500 mb over northwest Montana. The 300 mb upper-air chart showed a strong jet maximum located over eastern Washington state illustrated by the observed 95 knot wind at Spokane (GEG). Lifted Indices (LI) of zero or less were observed from west-central Montana southwest into Idaho. Specifically, the 1200 UTC sounding at GTF indicated an LI of -1.

By 0000 UTC on 4 August, conditions had become more favorable for severe convection across Montana. The composite analysis (Fig. 3) at 0000 UTC showed several parameters converging across southern Alberta and north-central Montana. The surface frontal boundary was located east of a line from Lethbridge, Alberta (YQL) to GTF and extended south to Bozeman, Montana (BZN). Surface dew points remained above 50°F across portions of central and eastern Montana with dew points greater than 55°F across north-central Montana. The southeasterly jet maximum of 25 knots at 850 mb remained across eastern Montana, as did the thermal ridge over southern Alberta, western Montana, and into western Utah. The positively tilted short-wave trough at 700 mb was propagating east across western Manitoba and north-central Montana. Warming temperatures in the lower layers of the atmosphere combined with cooling aloft associated with the thermal trough at 500 mb advecting eastward, resulted in steepening lapse rates across north-central Montana. This contributed to a more favorable environment for severe convection by increasing potential instability. A 50 knot mid-level jet was also apparent moving across the central portions of Montana. The upper-level jet

maximum at 300 mb, previously located over eastern Washington state, was now over western Montana (the 0000 UTC 4 August GTF sounding indicated a 79 knot wind at the 300 mb level). The jet maximum helped to create favorable speed shear north of the jet axis, and the left front quadrant of the jet maximum was placed across north-central Montana. McGinley (1986) and others note that this region is favorable for enhancing upward motion through the ageostrophic secondary circulation.

Through the use of the composite charts (Figs. 2 and 3), the forecaster is now aided in visualizing the changing dynamic and thermodynamic structure of the atmosphere. This can help in narrowing down a region favorable for strong or severe thunderstorm development. In this particular case, the composite charts indicated north-central Montana as the area most conducive to severe weather.

III. SURFACE ANALYSIS

The 1800 UTC 3 August surface analysis (Fig. 4) showed dew points greater than 50°F extending from southern Alberta across central Montana with a 61°F dew point noted at YQL. A frontal boundary, east of the Continental Divide, extended from north-central to south-central Montana. By 0000 UTC, the front had moved east and was located just east of a line from YQL to GTF and south to BZN. This frontal boundary had similar characteristics associated with those of a Southern Plains dry line. Warm, dry air existed west of the surface boundary while a relatively cool, moist air mass prevailed east of the boundary. Dry air aloft and steep lapse rates aided in transferring momentum to the lower layers of the atmosphere which

contributed to the eastward progression of this boundary, as well as strengthening the moisture gradient found along it. The dew point at GTF decreased 18°F during the six-hour period from 1800 UTC to 0000 UTC as dry northwesterly winds began to advance south along the east slopes of the Rocky Mountains. Between 1800 UTC and 0000 UTC, moisture pooled over north-central Montana and southern Alberta, as illustrated by the position of the 55°F isodrosotherm. As noted by Johns and Hirt (1987), increased low-level moisture contributes to greater positive buoyancy for a lifted parcel and lowers the level of free convection (LFC). This decreases the amount of dynamically induced lift necessary to initiate and sustain deep convection. The moisture gradient east of the Rocky Mountains continued to increase as noted on the 0000 UTC 4 August surface analysis (Fig. 5). A dew point difference of 16°F existed between GTF and HVR as the drier, low-level air continued to filter southeast along the Continental Divide.

The intrusion of drier air along the east slopes of the Rocky Mountains alerts the forecaster that this area has a decreased threat for the development of severe convection. Thus, the focal point of the operational meteorologist shifts to the area where the higher concentration of low-level moisture exists.

IV. THETA-E ANALYSES

A 700 mb theta-e ridge (Fig. 6) at 1200 UTC on 3 August extended from Edmonton, Alberta (WEG) to GTF and south to Lander, Wyoming (LND). Last (1992) pointed out that equivalent potential temperature (theta-e) analyses are useful in locating areas of high

Convective Available Potential Energy (CAPE). A favored area for the formation of severe convective development, as noted by Campbell (1991), is along a theta-e axis. The 0000 UTC 4 August 700 mb theta-e analysis (Fig. 7) indicated the theta-e ridge axis had now shifted into eastern Montana, enhancing the potential for severe thunderstorms.

V. SOUNDING AND HODOGRAPH DATA

The 1200 UTC 3 August GTF sounding (Fig. 8) showed marginal instability with the Showalter and Lifted Indices both indicating values of -1. Mielke's (1979) local program for measuring CAPE, computed 1,920 J/kg of buoyant energy in the sounding. The GTF hodograph (Fig. 9) showed significant veering in the wind field and increasing speeds from the surface through 9,000 feet (MSL). This type of hodograph favors the development of cyclonically rotating, right-moving supercells (Doswell 1990).

The 0000 UTC GTF sounding on 4 August (Fig. 10) showed the atmosphere had stabilized in the past 12 hours as the lowest layers had dried considerably. This corresponded to the drier air found west of the frontal boundary. The Showalter and Lifted Indices were now +1 and +2, respectively. The threat for severe weather had now shifted east where the sharp dew-point gradient existed. The 0000 UTC GTF hodograph on 4 August (Fig. 11) showed a noticeable change in the structure of the wind field. Winds from the surface to about 8,000 feet (MSL) prevailed from the northwest compared to the previous 12 hours where a southerly component to the winds existed.

VI. BULK RICHARDSON NUMBER

Severe weather can result from any type of convective storm, however certain storm types are more likely to produce severe weather than others. Being able to determine what type of convective storm may result from a given environment can be a valuable tool in this assessment. One such tool, the Bulk Richardson Number (BRN), is a relationship between wind shear and buoyancy. Observations and research from Weisman and Klemp (1986) suggest the BRN can be related to a preferred storm type. The BRN (R) is expressed by:

$$R = \frac{B}{1/2U^2}$$

where B is the buoyant energy in the storm's environment (CAPE) and U is a density weighted mean measure of the vertical wind shear through a relatively deep layer (0-6 km AGL). Lazarus and Droegemeier (1990) point out that the BRN is a bulk measure of the ambient shear and does not account for detailed aspects of the wind profile, particularly low-level veering. The results obtained by Weisman and Klemp, in their numerical studies of convective storms, noted that for unsteady, multicellular storm growth, values of R were greater than 30. For isolated supercellular storm growth, values of R ranged between 10 and 40.

Weisman and Klemp (1986) note that although the magnitude of R may indicate a preferred cell type to be favored in a given region, it does not necessarily provide an indication to the severity of that convection. An example of this is an environment with small buoyant energy ($B < 1000 \text{ m}^2/\text{s}^2$) and

moderate 0-6 km wind shear ($4 \times 10^{-3} \text{ s}^{-2}$). The value of R may be well within the range for supercell development, and a forecaster would then expect some of the convective storms to have the steadiness and propagation characteristics of supercell storms. However, since other factors are also important for severe convective development, one cannot be assured that given the existence of a supercell, severe weather will occur (Johns and Doswell 1992). Also, an environment with large buoyant energy ($B > 3500 \text{ m}^2/\text{s}^2$) and moderate 0-6 km wind shear may be characterized by a relatively large value of R , yet produce tornadoes or large hail with a relatively unsteady, or cyclic storm.

In the case on 3 August, the 1200 UTC hodograph at GTF (Fig. 9) had an observed BRN value of 28 which is in the range determined by Weisman and Klemp for isolated supercell storm structure. As mentioned earlier, the buoyant energy at GTF was 1,920 J/kg and considerable wind shear was evident from the hodograph. This diagnosis can aid the forecaster in assessing not only if the threat of severe weather exists, but what type of storm structure will or should occur.

The 0000 UTC 4 August GTF hodograph (Fig. 11) indicated a BRN value of 2, which did not fit into either category of multicellular or isolated supercell storm type. The influence of the dry, low-level northwesterly winds along the east slopes of the Rocky Mountains significantly altered the buoyancy and wind shear terms of the BRN equation.

However, by modifying the low-level conditions (e.g., surface to 700 mb) of the GTF sounding to those near HVR in north-central Montana, a proximity

sounding representing conditions near the area of possible severe weather can be constructed. This is achieved by substituting the surface data from HVR for GTF, and then interpolating values from the upper-air data at 850 mb and 700 mb. Through the substitution of these data, a modified HVR sounding and hodograph was constructed using the SHARP Workstation (Hart and Korotky 1991). The 0000 UTC 4 August modified sounding for HVR indicated a positive buoyant energy of $2170 \text{ m}^2/\text{s}^2$ (Fig. 12). The modified HVR hodograph (Fig. 13) produced a BRN of 24, which indicated an environment conducive for isolated supercell storm structure and development. Satellite photos (not shown) indicated that an isolated supercell developed over north-central Montana and moved south-southeast (330°). This movement was noticeably to the right of the 0-6 km mean wind (252°). This cell was responsible for the production of large hail and an F0 tornado.

VII. HELICITY

Although the BRN is a useful parameter, it is not as detailed of a predictor of storm rotation because it is a bulk measure and does not take into account details of the vertical wind profile. In recent years, special emphasis has been placed on the lowest 2 or 3 km of the atmosphere, usually below the level of free convection (LFC), which is considered the inflow layer into a convective storm. Storm relative helicity (Davies-Jones 1990) is an important parameter used to measure the potential storm rotation obtainable for a given environmental low-level wind field. Storm relative helicity (SRH) is the summation of the streamwise vorticity

through the storm inflow layer and indicates the rotation potential of a thunderstorm updraft. In other words, air parcels flowing toward the updraft region of a thunderstorm spin about a horizontal vorticity axis. When lifted into the updraft, this axis is tilted and stretched into the vertical and develops a cyclonic rotation.

SRH is calculated on the SHARP Workstation as twice the area bounded by the hodograph between the storm inflow vectors at the top and bottom of the measured layer. SHARP uses an initial storm motion of 30 degrees to the right of the 0-6 km mean wind, and 75 percent of its magnitude (after Leftwich 1990) to get an estimate of the SRH. This would allow the forecaster an initial first guess as to the amount of SRH available in a given environment before the storms develop. Then, storm motion can easily be updated on the SHARP Workstation with the use of radar data, for example. In a study of 28 tornado cases, Davies-Jones (1990) found approximate ranges of 0-3 km (AGL) SRH corresponding to tornado intensity. For weak tornadoes (F0-F1), helicity values were between $150\text{-}299 \text{ m}^2/\text{s}^2$ while for strong tornadoes (F2-F3), helicity values ranged from $300\text{-}449 \text{ m}^2/\text{s}^2$. Violent tornadoes (F4-F5) produced helicity values greater than $450 \text{ m}^2/\text{s}^2$.

Calculations of SRH were made by using the modified hodograph in section 6 and modifying the observed storm motion. Storm motion, initially calculated by the SHARP Workstation, indicated a storm motion of 286 degrees at 14 knots and a SRH of $157 \text{ m}^2/\text{s}^2$ (Fig. 13). Using the observed radar data, a storm motion of 330 degrees at 15 knots was substituted for the SHARP Workstation storm motion. Given these modifications, the 0-

3 km SRH was $221 \text{ m}^2/\text{s}^2$ (Fig. 14) which is a considerable increase over the initial calculation of SRH. The increased SRH shows a greater rotation potential of the thunderstorm updraft.

VIII. CONCLUSIONS

Severe convection initiated as a result of several key parameters: low-level moisture ahead of a sharpening moisture gradient as a front moved east into the HVR area; low-level convergence and a 700 mb short-wave trough were present to provide dynamical forcing of the moist air; a thermal trough at 500 mb aided in destabilizing the atmosphere as mid-level cold air advection advanced into north-central Montana; the left front quadrant of a 300 mb jet maximum supported upward motion; and moderate values of buoyant energy existed. Composite analysis proved useful to graphically show all of the above features. This aided the forecaster in isolating north-central Montana as the area most favored for severe weather.

The Bulk Richardson Number was utilized to assess the predicted type of storm structure for this particular environment. Modifications made to the sounding and hodograph data using the HVR surface and low-level observations, via the SHARP Workstation, led to a more accurate assessment of potential buoyant energy and vertical wind shear in the convective area. Storm relative helicity provided even further information about the low-level inflow (0-3 km AGL) into a convective storm and its potential to generate cyclonic rotation and long-lived supercell thunderstorms.

The forecaster may want to consider modification of the surface and upper-air

data features in close proximity to the severe weather threat area to derive a better representation of the near storm environment. As in the above case, this can be a very valuable tool to forecasters.

IX. ACKNOWLEDGMENTS

I would like to thank John Mecikalski (University of Wisconsin) and Bob Johns (NSSF) for their valuable insight into this project as well as Jeff Last (WSFO MKX) for his assistance with some of the modifications made on the SHARP Workstation.

X. REFERENCES

- Campbell, M., 1991: Equivalent potential temperature (θ_e) applications. *Western Region Technical Attachment 91-37*, NWS Western Region, Scientific Services Division, Salt Lake City, Utah.
- Davies-Jones, R., D. Burgess, and M. Foster, 1990: Test of helicity as a tornado forecast parameter. *Preprints, 16th Conference on Severe Local Storms*, Kananaskis Park, Alberta, Amer. Meteor. Soc. 588-592.
- Doswell, C. A. III, 1990: On the use of hodographs: vertical wind profile information applied to forecasting severe thunderstorms. *Training Notes*, NWS Southern Region Headquarters, 37 pp.
- Hart, J. A., and W. Korotky, 1991: The SHARP Workstation v1.50. A SkewT-hodograph research program for the IBM and compatible PC. NOAA/NWS, Charleston, West Virginia, 30 pp.

Johns, R. H., and W. D. Hirt, 1987:
Derechos: widespread convectively
induced windstorms. *Wea. Fcst.*, 2, 32-49.

Johns, R. H., and C. A. Doswell III, 1992:
Severe local storm forecasting. *Preprints,
Symposium on Weather Forecasting*,
Atlanta, Georgia, American
Meteorological Society, 225-236.

Last, J. K., 1992: Examples of significant
thunderstorm initiation in identifiable
low level theta-e patterns. *Central
Region Technical Attachment*, NWS
Central Region, Scientific Services
Division, Kansas City, Missouri.

Lazarus, S. M., and K. K. Droegemeier,
1990: The influence of helicity on the
stability and morphology of numerically
simulated storms. *Preprints, 16th
Conference on Severe Local Storms*,
Kananaskis Park, Alberta, Amer. Meteor.
Soc., 269-274.

McGinley, J., 1986: Nowcasting Mesoscale
Phenomena. *Mesoscale Meteorology and
Forecasting*, (P. S. Ray, ed.), Amer.
Meteor. Soc., 657-688.

Mielke, K. B., 1979: A computer program
for convective parameters. *Natl. Wea.
Dig.*, Volume 4, Number 3, 10-18.

Weisman, M. L., and J. B. Klemp, 1982:
The dependence of numerically simulated
convective storms on vertical wind shear
and buoyancy. *Mon. Wea. Rev.*, 110, 504-
520.

Weisman, M. L., and J. B. Klemp, 1984:
The structure and classification of
numerically simulated convective storms
in directionally varying wind shears.
Mon. Wea. Rev., 112, 2479-2498.

Weisman, M. L., and J. B. Klemp, 1986:
Characteristics of isolated convective
storms. *Mesoscale Meteorology and
Forecasting*, (P. S. Ray, ed.), Amer.
Meteor. Soc., 331-358.

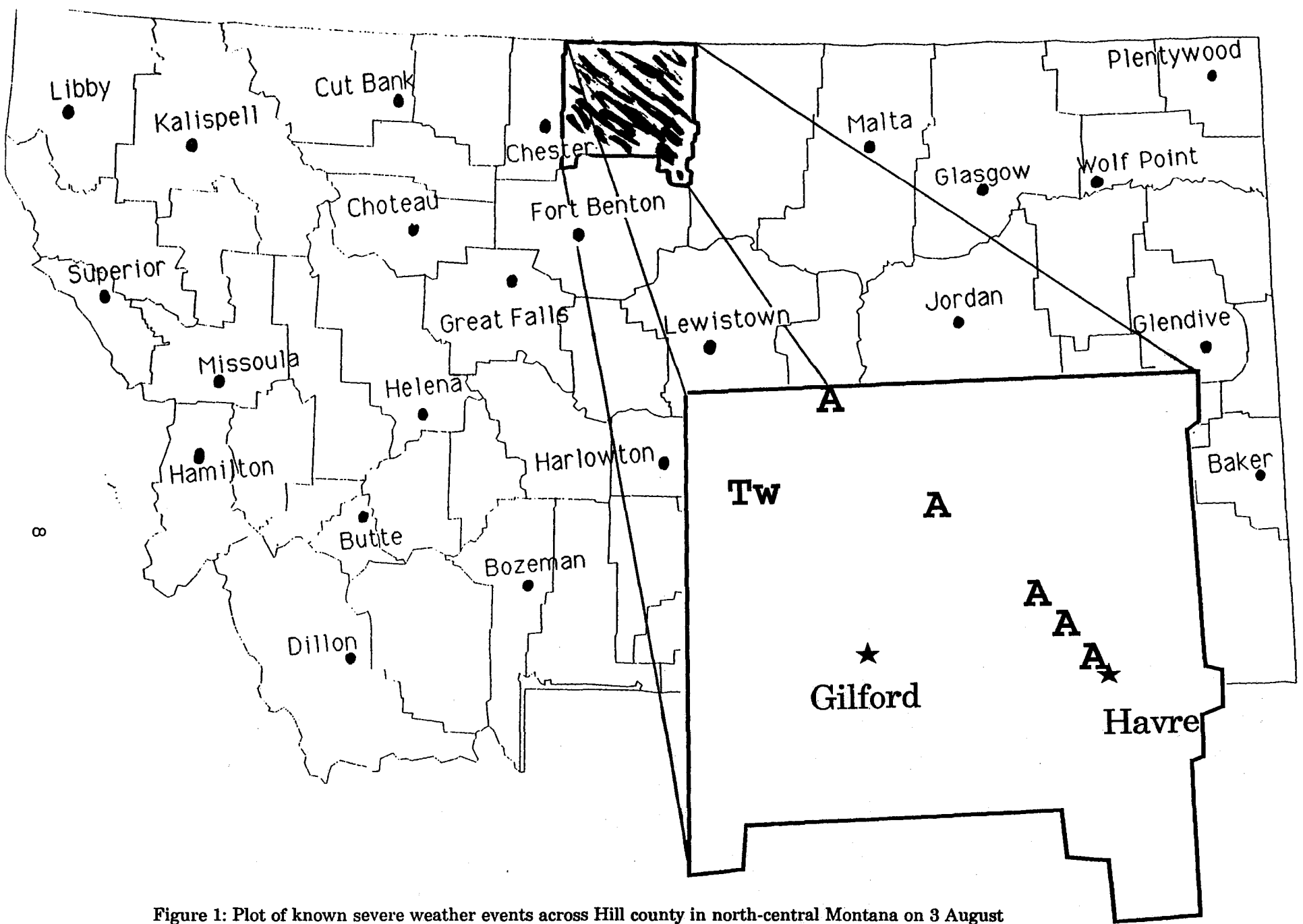


Figure 1: Plot of known severe weather events across Hill county in north-central Montana on 3 August 1992. (Reports from Storm Data and local storm reports.) T = tornado W = wind damage
 A = hail greater than 3/4 inch diameter.

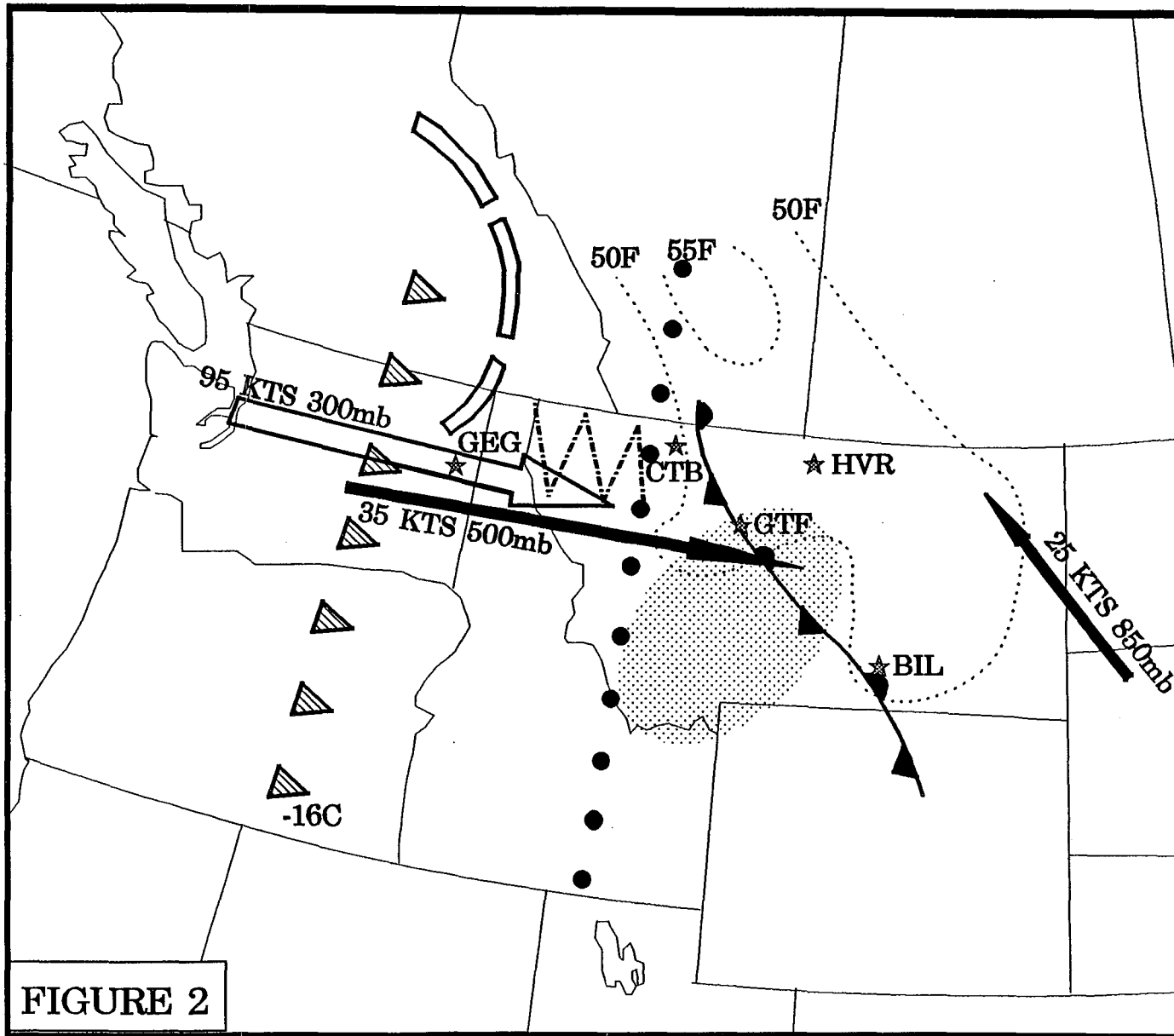


Figure 2: Composite analysis at 1200 UTC on 3 August 1992. Arrow represent jet maxima at various levels. Dotted line represents the 850 mb thermal ridge. Large dashed line denotes 700 mb short wave trough. Triangular line indicates thermal trough at 500 mb. Jagged dot-dashed line represents diffuence at the 500 mb level. Thin dashed lines represent surface isodrosotherms analyzed every 5° F (>50° F). Stippled area denotes Lifted Indices less than or equal to zero.

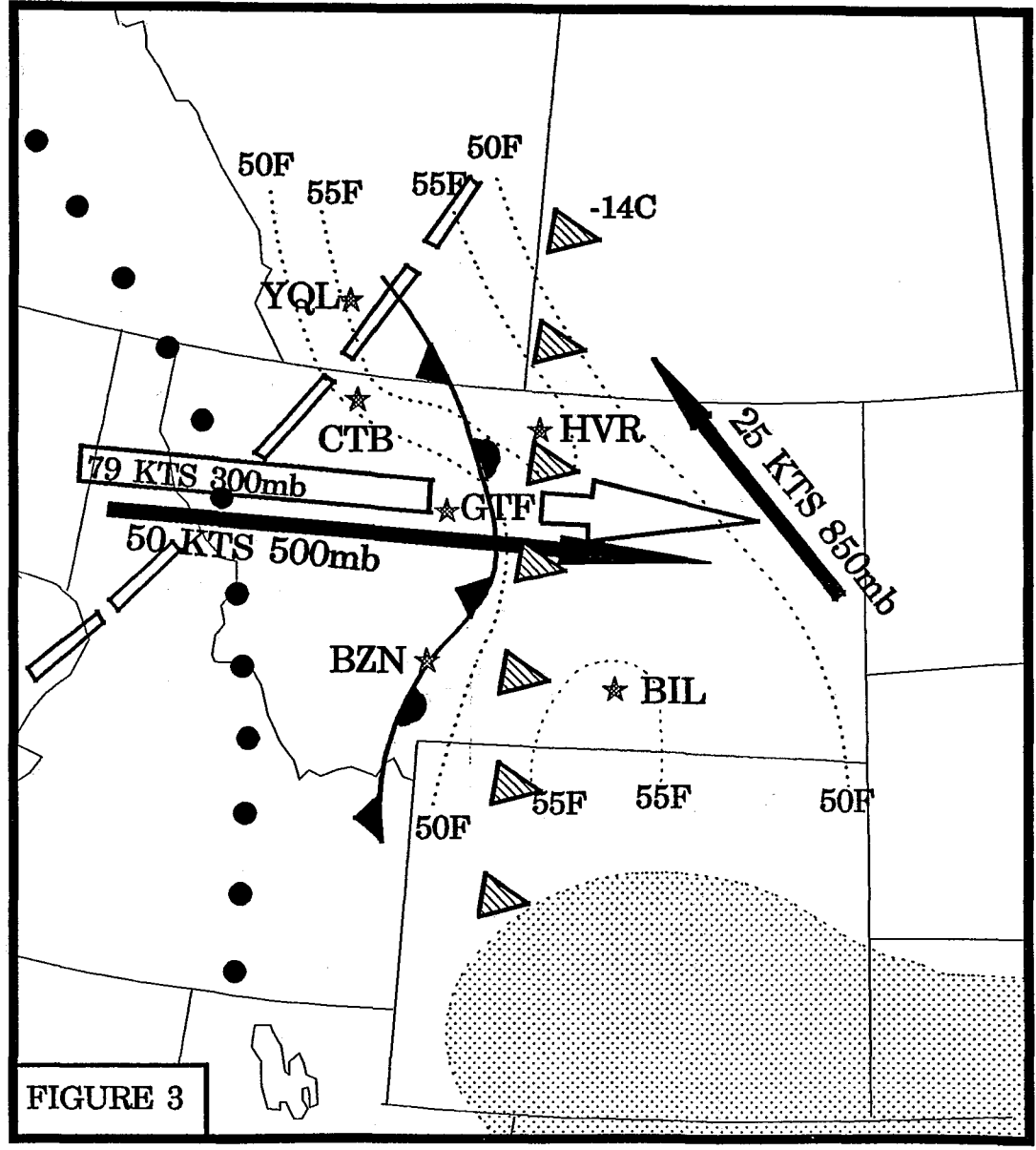


Figure 3: Same as Figure 2 except at 0000 UTC on 4 August 1992.

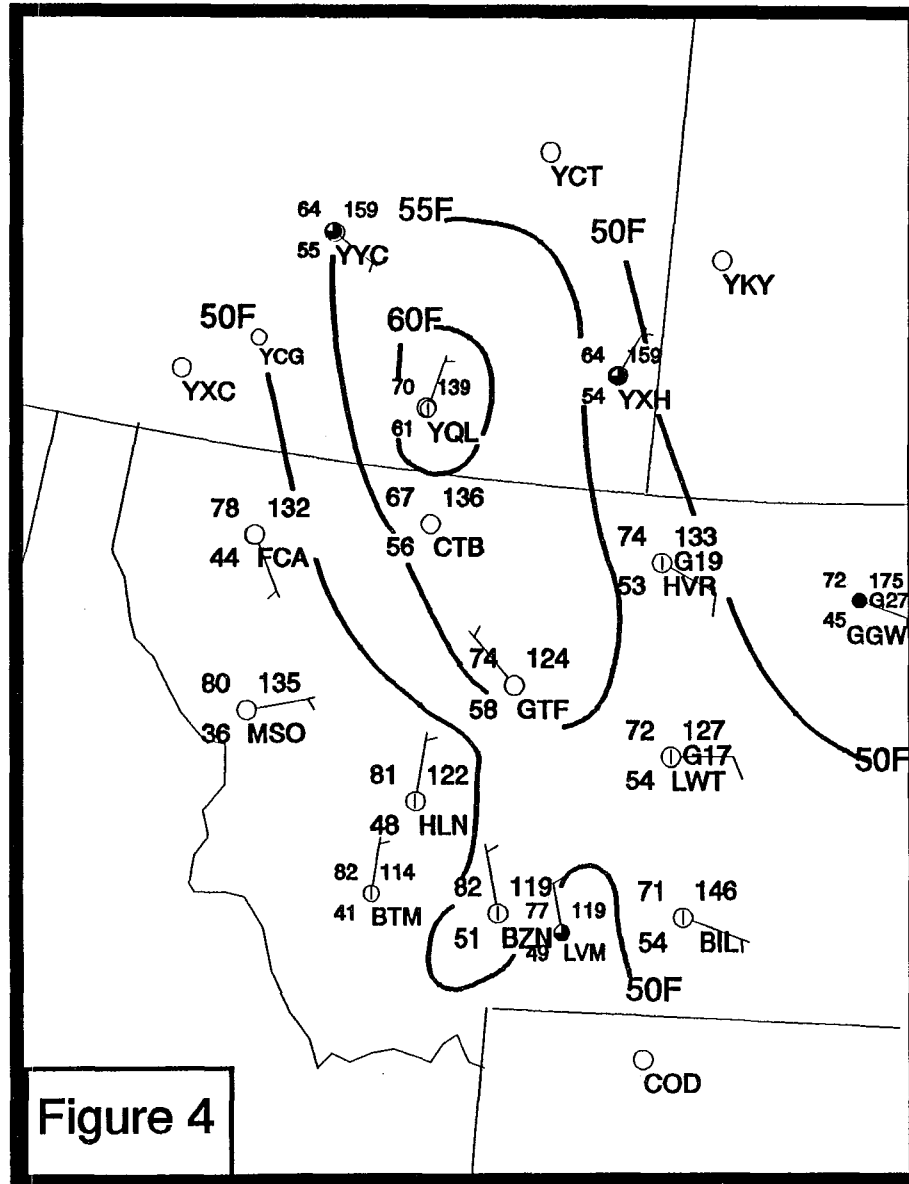


Figure 4: 1800 UTC surface analysis on 3 August 1992. Solid lines represent isodrosotherms analyzed every 5°F.

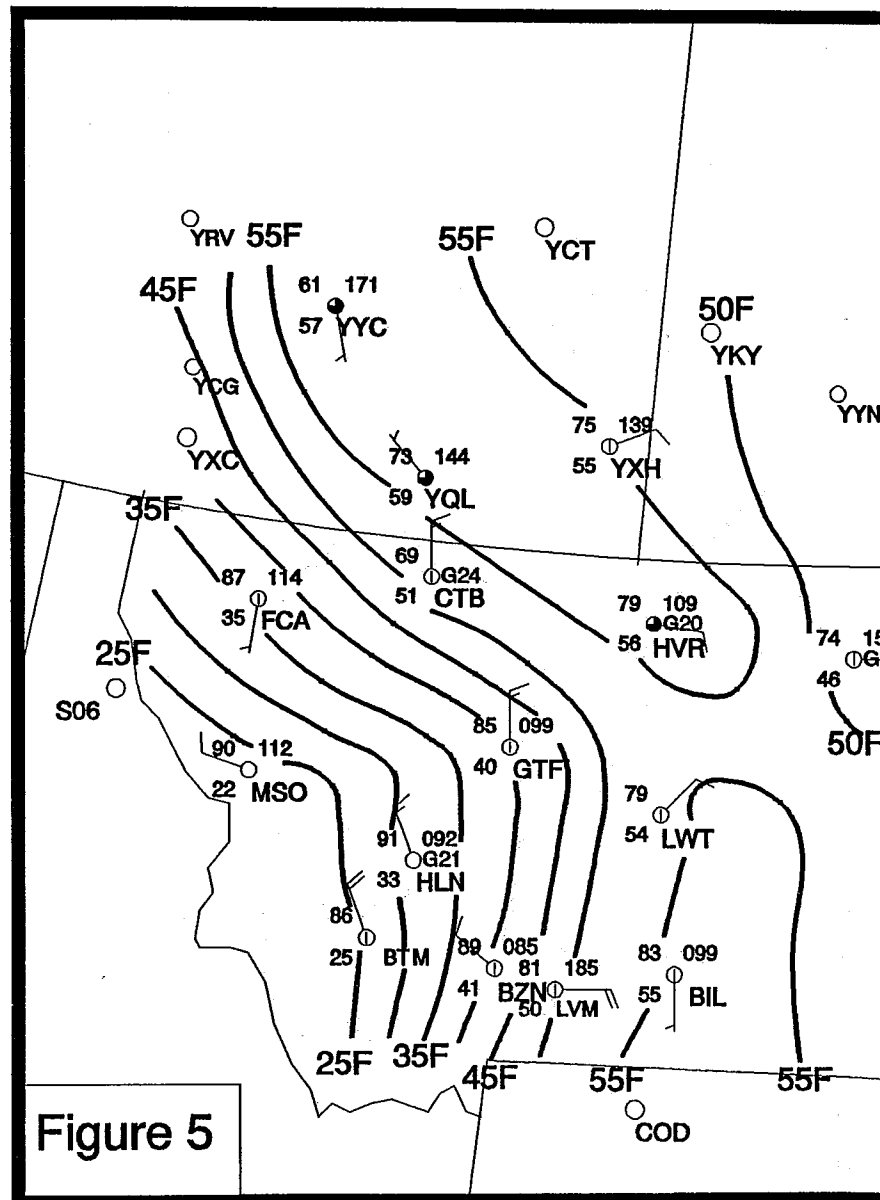


Figure 5: 0000 UTC surface analysis on 4 August 1992. Solid lines represent isodrosotherms analyzed every 5°F.

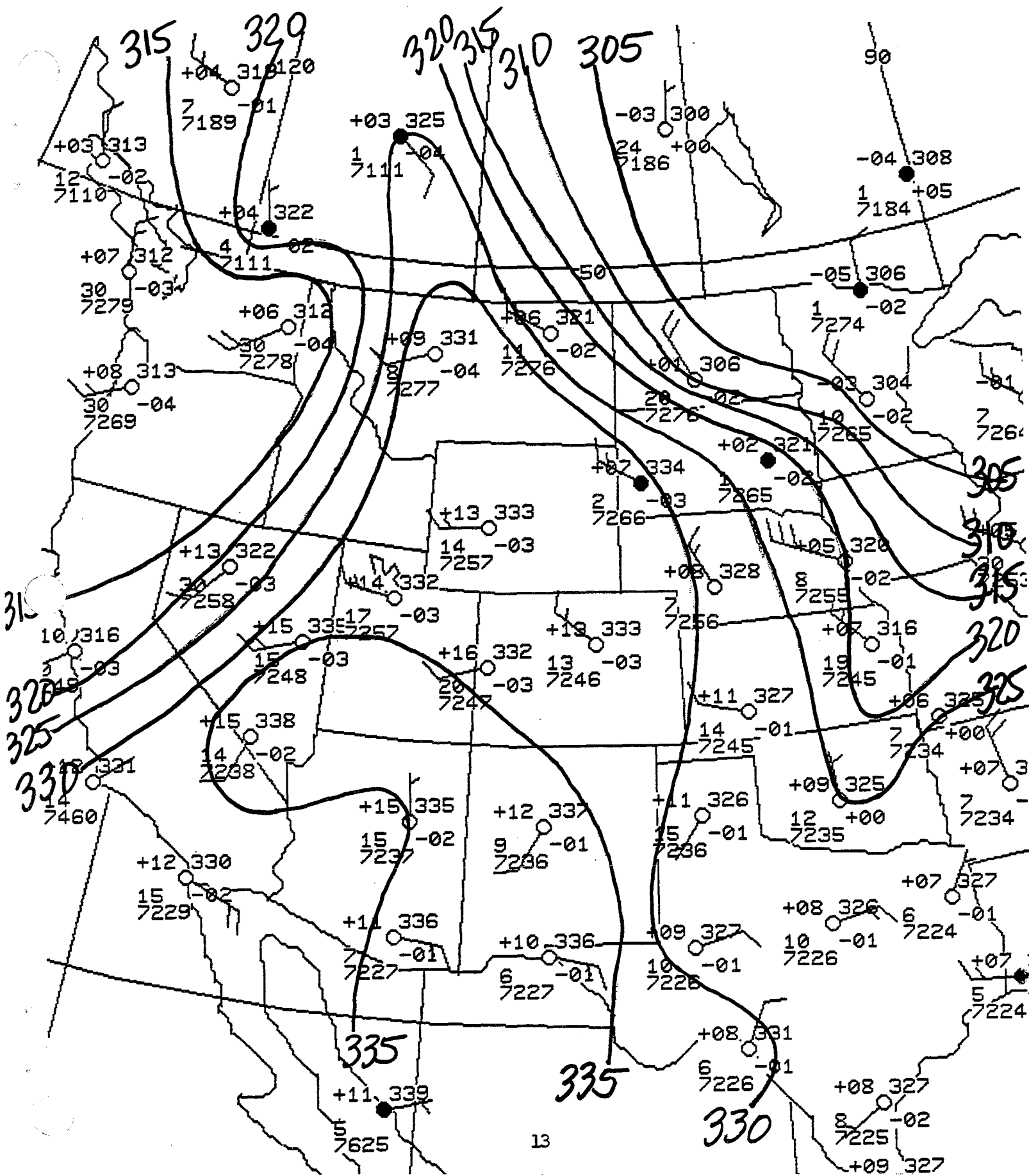


Figure 6: 1200 UTC 700 mb equivalent potential temperature analysis on 3 August 1992. Solid lines represent equivalent isentropes analyzed every 5K.

Figure 7: 0000 UTC 700 mb equivalent potential temperature analysis on 4 August 1992. Solid lines represent equivalent isentropes analyzed every 5K.

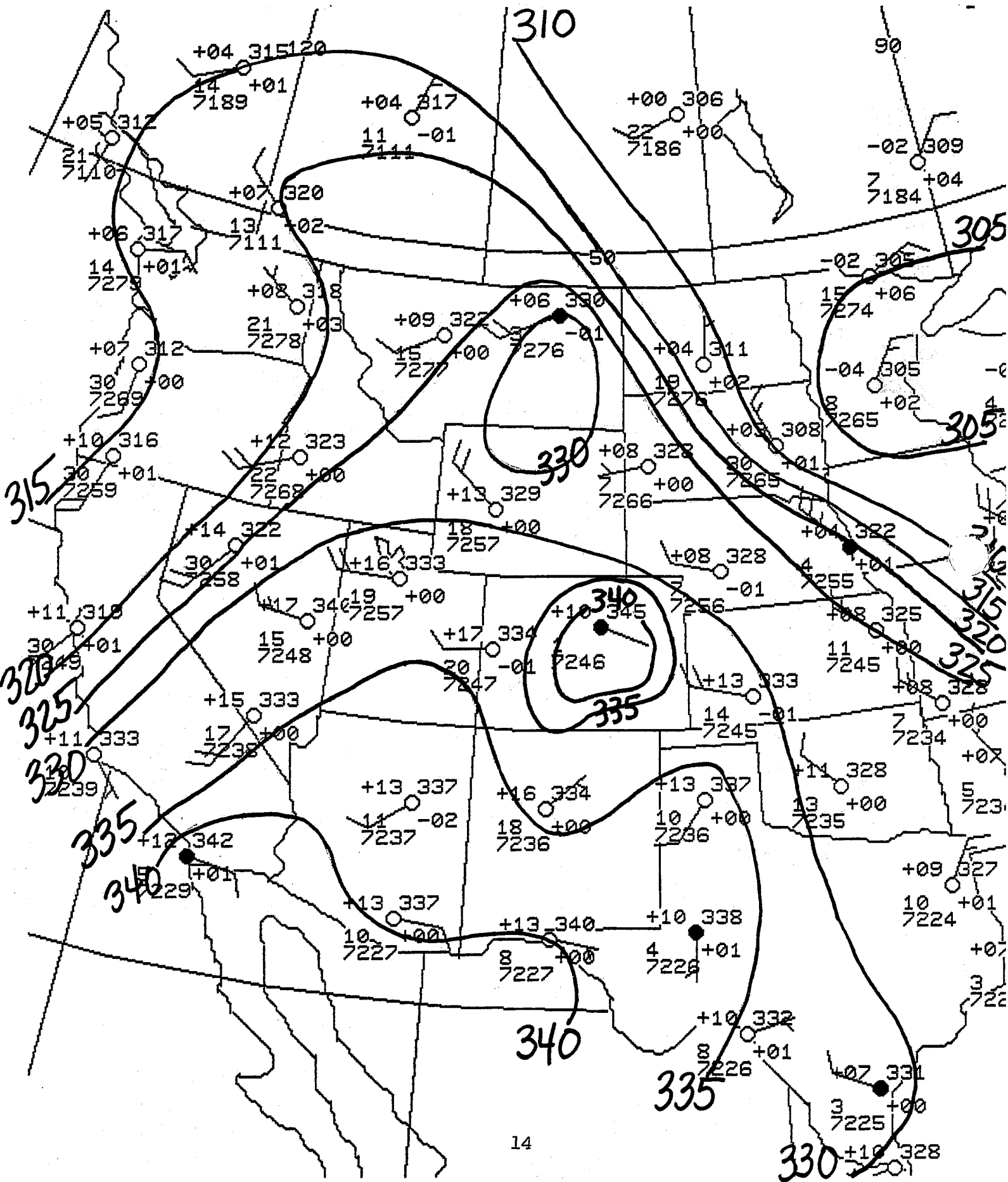
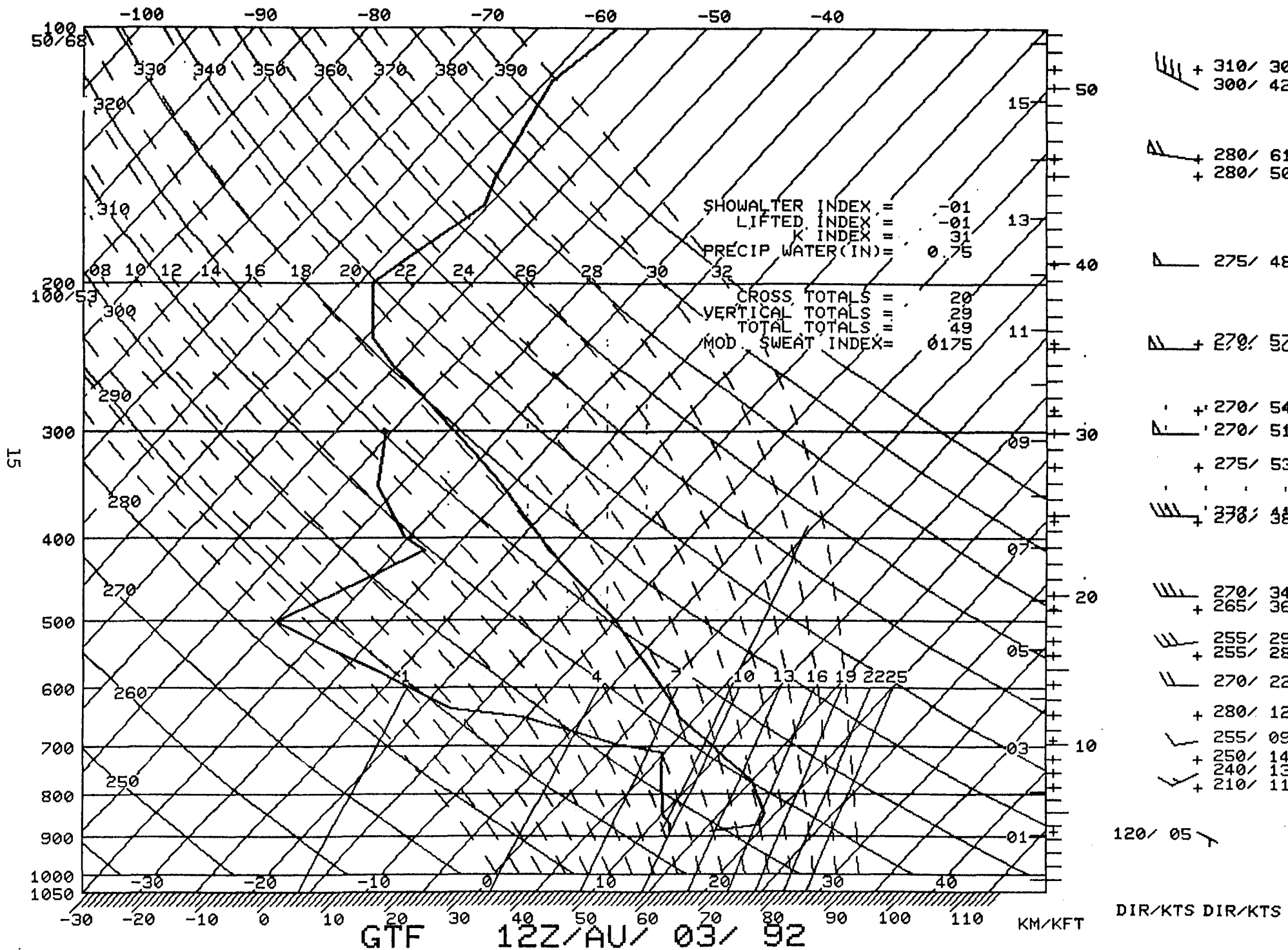


Figure 8: 1200 UTC Great Falls, Montana (F) SkewT-logP sounding on 3 August 1992.



GTF 12Z 3 AUG 92

B R N = 28
 B+ = 161 (M/SEC)**2 X 10
 B- = 0 (M/SEC)**2 X 10
 SHR = 58 (M/SEC)**2
 WMAX = 57 M/SEC
 EL = 197 MB, 402 HND FT
 MPL = 489 HND FT
 VS5 = 7 (M/SEC)**2
 SS15 = 68 10-4 SEC-1

UNITS : KNOTS, LVLS : THSD FT (MSL)

PARCEL FROM PMAX
 ENTRAINMENT = 60 PERCENT
 P0 = 888 MB
 PMAX = 771 MB
 LCL = 679 MB
 LFC = 511 MB

EI = -2 J/KG X 10
 EI+ = 6 (+ PART)
 EI- = -7 (- PART)

ENERGY CHANGE IN LAYERS

P1	P2	
771	511	-7 J/KG X 10
511	236	15
236	100	-472

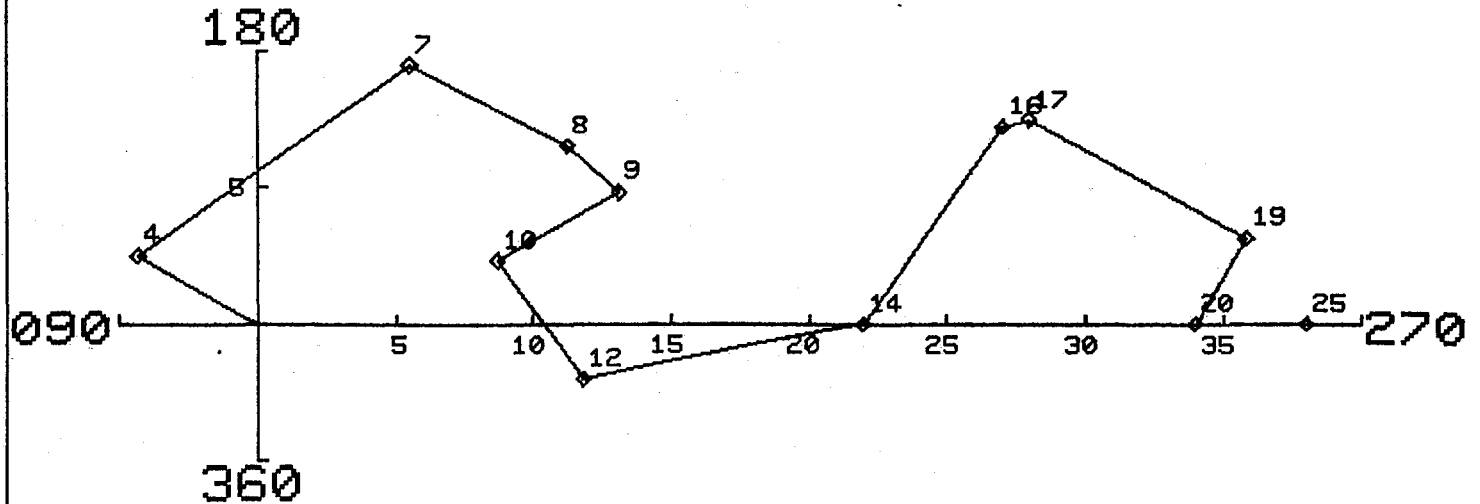


Figure 9: 1200 UTC Great Falls, Montana (GTF) hodograph on 3 August 1992 in ms^{-1} . Points along the hodograph indicate thousands of feet (MSL).

LI = 0
 KI = 31
 SWI = -1

CCL = MB

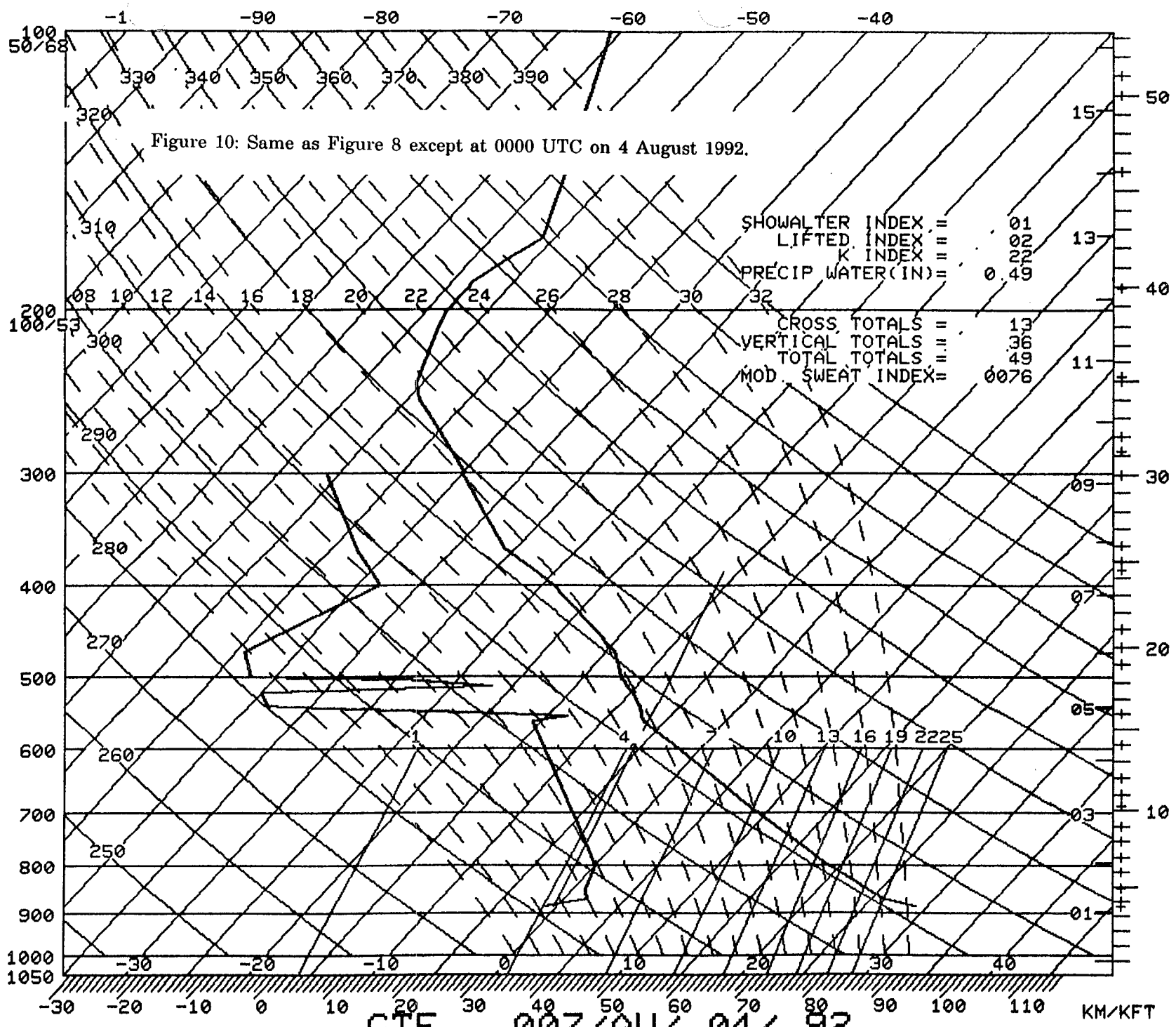


Figure 10: Same as Figure 8 except at 0000 UTC on 4 August 1992.

SHOWALTER INDEX = 01
 LIFTED INDEX = 02
 K INDEX = 22
 PRECIP WATER(IN) = 0.49
 CROSS TOTALS = 13
 VERTICAL TOTALS = 36
 TOTAL TOTALS = 49
 MOD. SWEAT INDEX = 0076

- 270/ 28
- + 270/ 29
- 285/ 39
- 275/ 60
- 278/ 83
- 270/ 84
- + 270/ 82
- 270/ 79
- + 270/ 54
- + 278/ 52
- + 270/ 51
- 275/ 50
- + 275/ 47
- 270/ 48
- + 260/ 31
- 245/ 22
- + 245/ 16
- + 249/ 13
- + 245/ 11
- 265/ 07
- 305/ 05
- 340/ 07
- 350/ 09
- 345/ 09
- 345/ 07
- 340/ 06

GTF 00Z/AU/ 04/ 92 KM/KFT

DIR/KTS DIR/KTS

GTF 00Z 4 AUG 92

UNITS : KNOTS, LVLS : THSD FT (MSL)

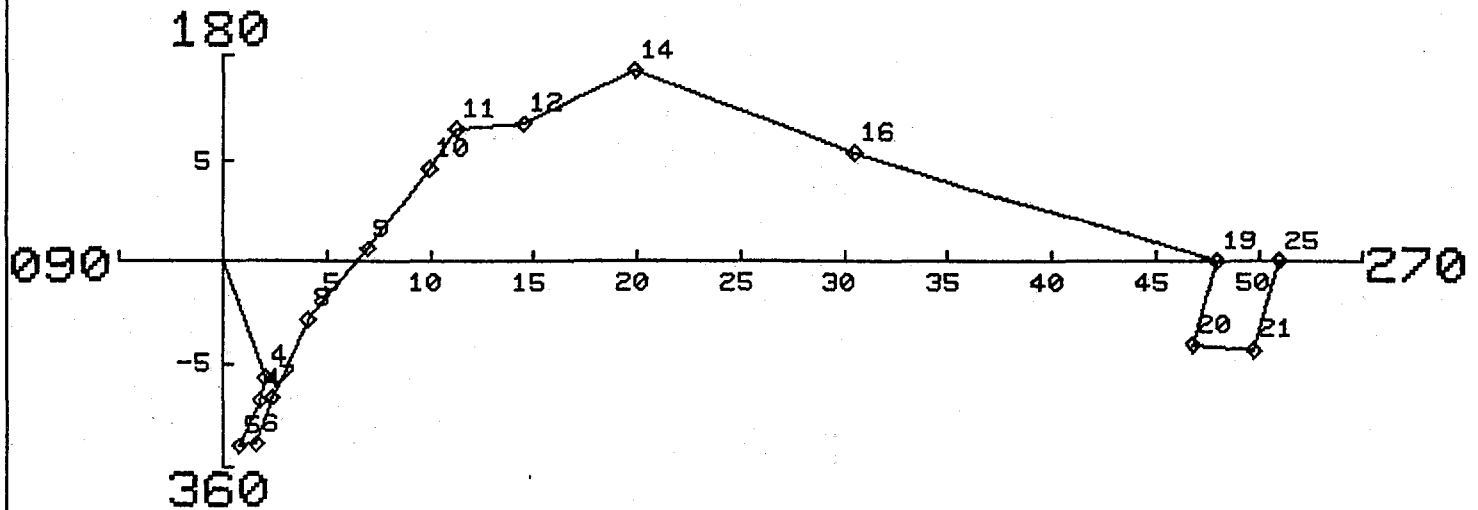
B R N = 2
 B+ = 12 (M/SEC)**2 X 10
 B- = 0 (M/SEC)**2 X 10
 SHR = 67 (M/SEC)**2
 WMAX = 16 M/SEC
 EL = 304 MB, 308 HND FT
 MPL = 365 HND FT
 VS5 = 0 (M/SEC)**2
 SS15 = 72 10-4 SEC-1

PARCEL FROM PMAX
 ENTRAINMENT = 60 PERCENT

P0 = 886 MB
 PMAX = 869 MB
 LCL = 595 MB
 LFC = -999 MB

EI = -30 J/KG X 10
 EI+ = 0 (+ PART)
 EI- = -30 (- PART)

ENERGY CHANGE IN LAYERS
 P1 P2
 869 100 -679 J/KG X 10



LI = 1
 KI = 22
 SWI = 1

Figure 11: Same as Figure 9 except at 0000 UTC on 4 August 1992.

CCL = 579 MB
 C TMP = 30 C, 86 F
 WAVG = G/KG X 10-1

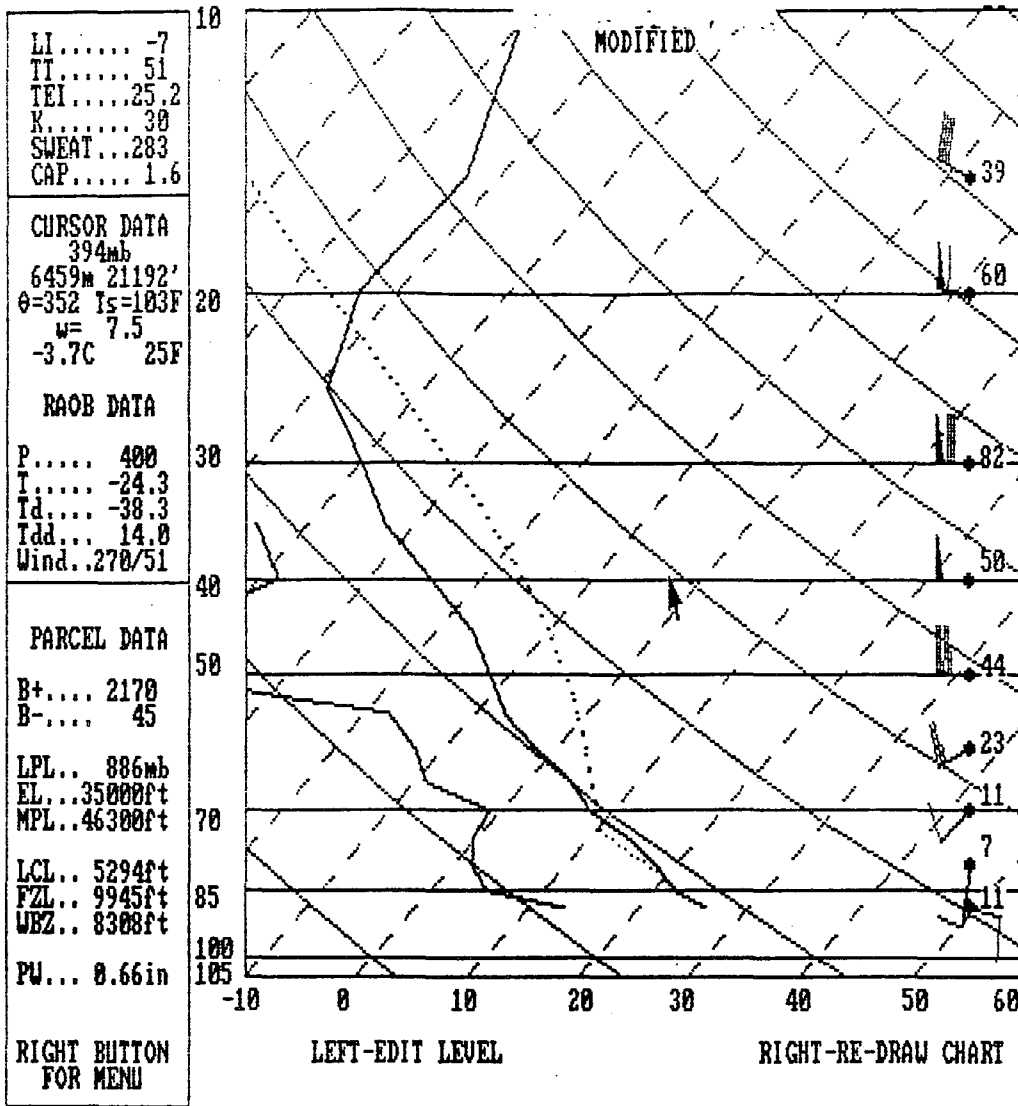


Figure 12: 0000 UTC 4 August 1992 modified SkewT-logP sounding for Havre, Montana (HVR) via the SHARP Workstation.

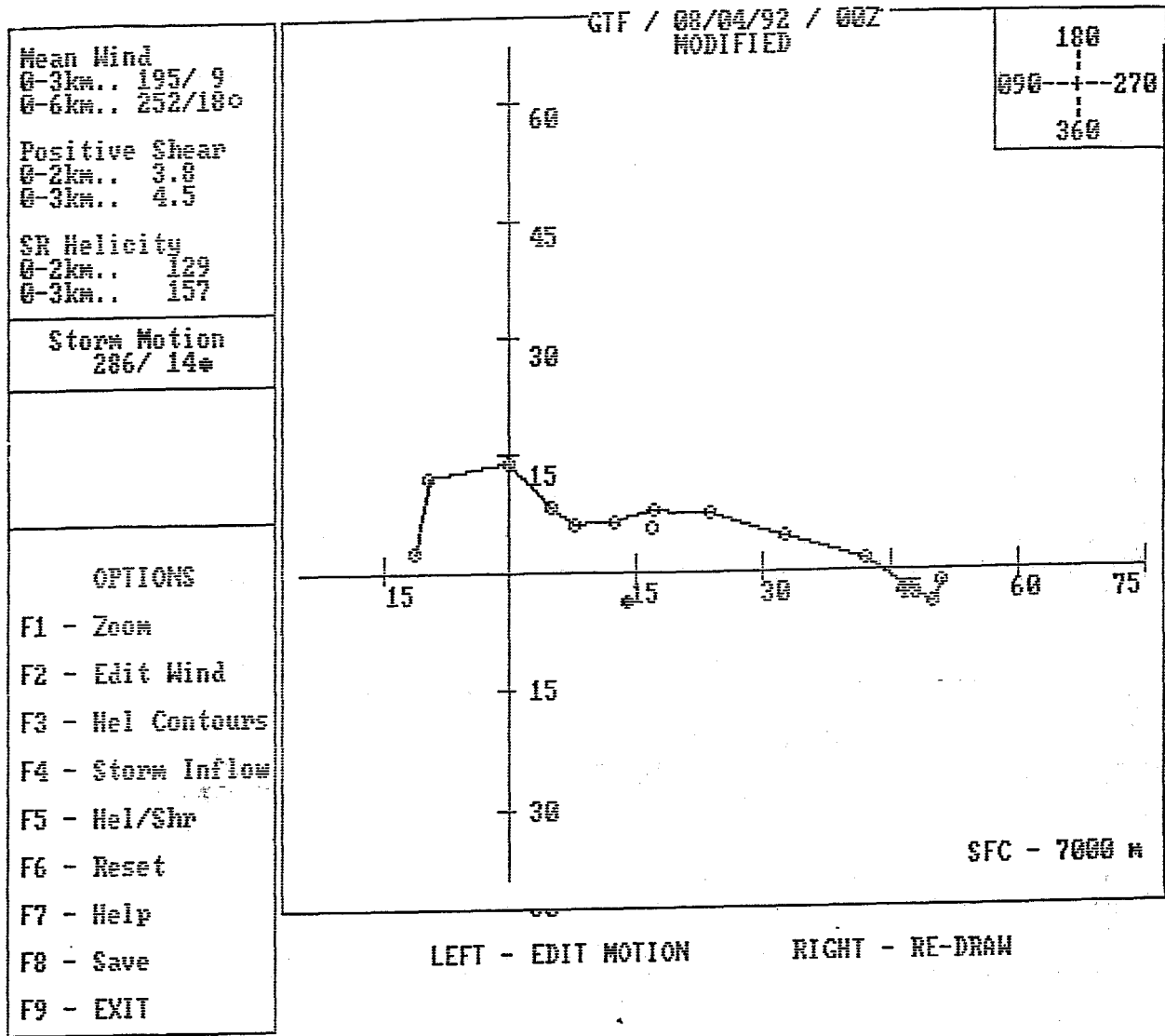


Figure 13: 0000 UTC 4 August 1992 modified hodograph for Havre, Montana (HVR) via the SHARP Workstation using the default storm motion (70% of the magnitude and 30° to the right of the 0-6 km mean wind).

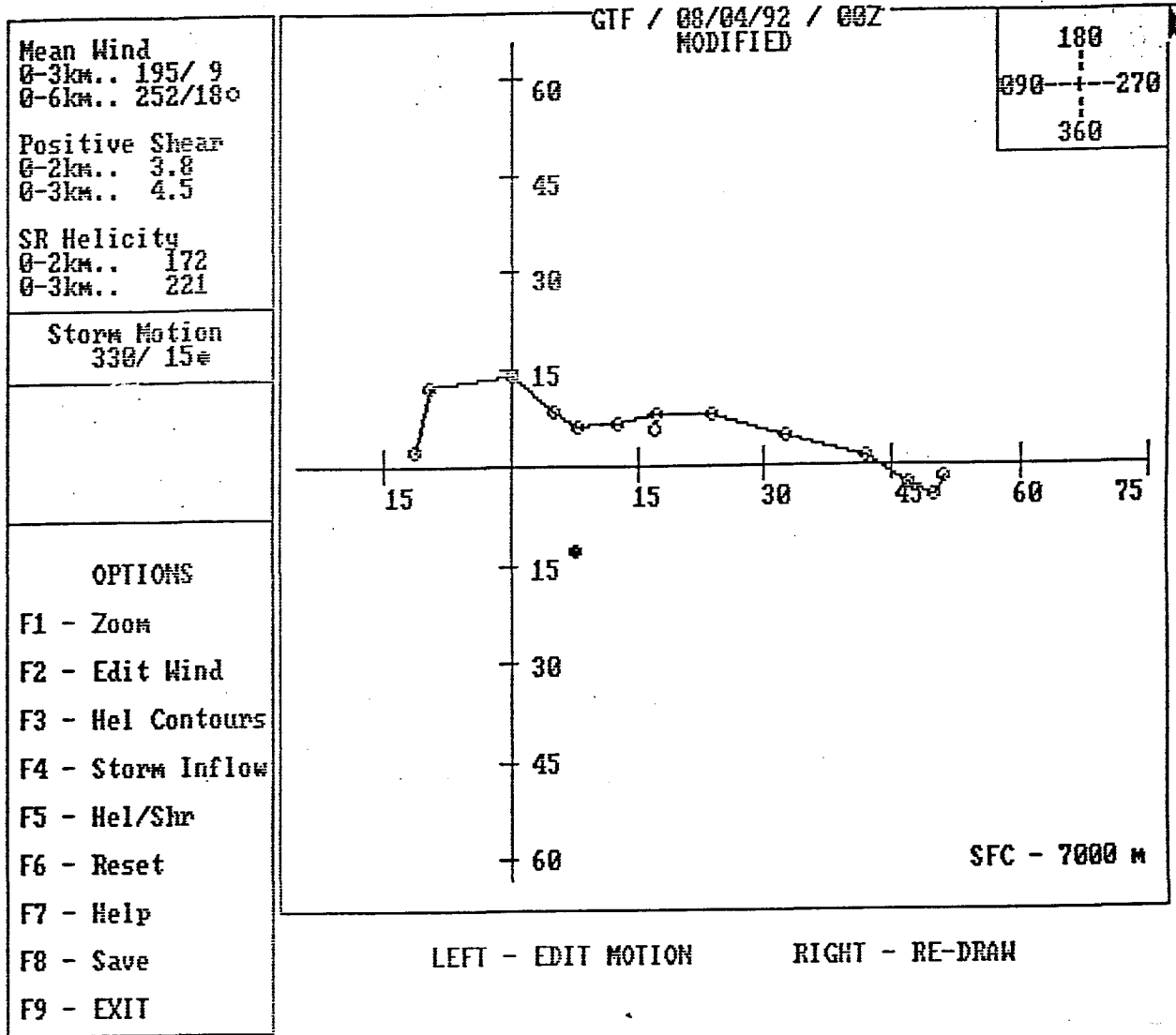


Figure 14: 0000 UTC 4 August 1992 modified Havre, Montana (HVR) hodograph using the observed storm motion from radar data.

- 142 The Usefulness of Data from Mountaintop Fire Lookout Stations in Determining Atmospheric Stability. Jonathan W. Corey, April 1979. (PB298899/AS)
- 143 The Depth of the Marine Layer at San Diego as Related to Subsequent Cool Season Precipitation Episodes in Arizona. Ira S. Brenner, May 1979. (PB298817/AS)
- 144 Arizona Cool Season Climatological Surface Wind and Pressure Gradient Study. Ira S. Brenner, May 1979. (PB298900/AS)
- 146 The BART Experiment. Morris S. Webb, October 1979. (PB80 155112)
- 147 Occurrence and Distribution of Flash Floods in the Western Region. Thomas L. Dietrich, December 1979. (PB80 160344)
- 149 Misinterpretations of Precipitation Probability Forecasts. Allan H. Murphy, Sarah Lichtenstein, Baruch Fischhoff, and Robert L. Winkler, February 1980. (PB80 174576)
- 150 Annual Data and Verification Tabulation - Eastern and Central North Pacific Tropical Storms and Hurricanes 1979. Emil B. Gunther and Staff, EPHC, April 1980. (PB80 220486)
- 151 NMC Model Performance in the Northeast Pacific. James E. Overland, PMEL-ERL, April 1980. (PB80 196033)
- 152 Climate of Salt Lake City, Utah. Wilbur E. Figgins (Retired) and Alexander R. Smith. Fifth Revision, July 1992. (PB92 220177)
- 153 An Automatic Lightning Detection System in Northern California. James E. Rea and Chris E. Fontana, June 1980. (PB80 225592)
- 154 Regression Equation for the Peak Wind Gust 6 to 12 Hours in Advance at Great Falls During Strong Downslope Wind Storms. Michael J. Oard, July 1980. (PB91 108367)
- 155 A Raininess Index for the Arizona Monsoon. John H. Ten Harkel, July 1980. (PB81 106494)
- 156 The Effects of Terrain Distribution on Summer Thunderstorm Activity at Reno, Nevada. Christopher Dean Hill, July 1980. (PB81 102501)
- 157 An Operational Evaluation of the Scofield/Oliver Technique for Estimating Precipitation Rates from Satellite Imagery. Richard Ochoa, August 1980. (PB81 108227)
- 158 Hydrology Practicum. Thomas Dietrich, September 1980. (PB81 134033)
- 159 Tropical Cyclone Effects on California. Arnold Court, October 1980. (PB81 133779)
- 160 Eastern North Pacific Tropical Cyclone Occurrences During Intraseasonal Periods. Preston W. Leftwich and Gail M. Brown, February 1981. (PB81 205494)
- 161 Solar Radiation as a Sole Source of Energy for Photovoltaics in Las Vegas, Nevada, for July and December. Darryl Randerson, April 1981. (PB81 224503)
- 162 A Systems Approach to Real-Time Runoff Analysis with a Deterministic Rainfall-Runoff Model. Robert J.C. Burnash and R. Larry Ferral, April 1981. (PB81 224495)
- 163 A Comparison of Two Methods for Forecasting Thunderstorms at Luke Air Force Base, Arizona. LTC Keith R. Cooley, April 1981. (PB81 225393)
- 164 An Objective Aid for Forecasting Afternoon Relative Humidity Along the Washington Cascade East Slopes. Robert S. Robinson, April 1981. (PB81 23078)
- 165 Annual Data and Verification Tabulation, Eastern North Pacific Tropical Storms and Hurricanes 1980. Emil B. Gunther and Staff, May 1981. (PB82 230336)
- 166 Preliminary Estimates of Wind Power Potential at the Nevada Test Site. Howard G. Booth, June 1981. (PB82 127036)
- 167 ARAP User's Guide. Mark Mathewson, July 1981, Revised September 1981. (PB82 196783)
- 168 Forecasting the Onset of Coastal Gales Off Washington-Oregon. John R. Zimmerman and William D. Burton, August 1981. (PB82 127051)
- 169 A Statistical-Dynamical Model for Prediction of Tropical Cyclone Motion in the Eastern North Pacific Ocean. Preston W. Leftwich, Jr., October 1981. (PB82195298)
- 170 An Enhanced Plotter for Surface Airways Observations. Andrew J. Spry and Jeffrey L. Anderson, October 1981. (PB82 153883)
- 171 Verification of 72-Hour 500-MB Map-Type Predictions. R.F. Quiring, November 1981. (PB82 158098)
- 172 Forecasting Heavy Snow at Wenatchee, Washington. James W. Holcomb, December 1981. (PB82 177783)
- 173 Central San Joaquin Valley Type Maps. Thomas R. Crossan, December 1981. (PB82 196064)
- 174 ARAP Test Results. Mark A. Mathewson, December 1981. (PB82 198103)
- 176 Approximations to the Peak Surface Wind Gusts from Desert Thunderstorms. Darryl Randerson, June 1982. (PB82 253089)
- 177 Climate of Phoenix, Arizona. Robert J. Schmidl, April 1969 (Revised December 1986). (PB87 142063/AS)
- 178 Annual Data and Verification Tabulation, Eastern North Pacific Tropical Storms and Hurricanes 1982. E.B. Gunther, June 1983. (PB85 106078)
- 179 Stratified Maximum Temperature Relationships Between Sixteen Zone Stations in Arizona and Respective Key Stations. Ira S. Brenner, June 1983. (PB83 249904)
- 180 Standard Hydrologic Exchange Format (SHEF) Version I. Phillip A. Pasteris, Vernon C. Bissel, David G. Bennett, August 1983. (PB85 106052)
- 181 Quantitative and Spatial Distribution of Winter Precipitation along Utah's Wasatch Front. Lawrence B. Dunn, August 1983. (PB85 106912)
- 182 500 Millibar Sign Frequency Teleconnection Charts - Winter. Lawrence B. Dunn, December 1983. (PB85 106276)
- 183 500 Millibar Sign Frequency Teleconnection Charts - Spring. Lawrence B. Dunn, January 1984. (PB85 111367)
- 184 Collection and Use of Lightning Strike Data in the Western U.S. During Summer 1983. Glenn Rasch and Mark Mathewson, February 1984. (PB85 110534)
- 185 500 Millibar Sign Frequency Teleconnection Charts - Summer. Lawrence B. Dunn, March 1984. (PB85 111359)
- 186 Annual Data and Verification Tabulation eastern North Pacific Tropical Storms and Hurricanes 1983. E.B. Gunther, March 1984. (PB85 109635)
- 187 500 Millibar Sign Frequency Teleconnection Charts - Fall. Lawrence B. Dunn, May 1984. (PB85 110930)
- 188 The Use and Interpretation of Isentropic Analyses. Jeffrey L. Anderson, October 1984. (PB85 132694)
- 189 Annual Data & Verification Tabulation Eastern North Pacific Tropical Storms and Hurricanes 1984. E.B. Gunther and R.L. Cross, April 1985. (PB85 187887AS)
- 190 Great Salt Lake Effect Snowfall: Some Notes and An Example. David M. Carpenter, October 1985. (PB86 119153/AS)
- 191 Large Scale Patterns Associated with Major Freeze Episodes in the Agricultural Southwest. Ronald S. Hamilton and Glenn R. Lusk, December 1985. (PB86 144474AS)
- 192 NWR Voice Synthesis Project: Phase I. Glen W. Sampson, January 1986. (PB86 145604/AS)
- 193 The MCC - An Overview and Case Study on Its Impact in the Western United States. Glenn R. Lusk, March 1986. (PB86 170651/AS)
- 194 Annual Data and Verification Tabulation Eastern North Pacific Tropical Storms and Hurricanes 1985. E.E. Gunther and R.L. Cross, March 1986. (PB86 170941/AS)
- 195 Rapid Interpretation Guidelines. Roger G. Pappas, March 1986. (PB86 177690/AS)
- 196 A Mesoscale Convective Complex Type Storm over the Desert Southwest. Darryl Randerson, April 1986. (PB86 190998/AS)
- 197 The Effects of Eastern North Pacific Tropical Cyclones on the Southwestern United States. Walter Smith, August 1986. (PB87 106258AS)
- 198 Preliminary Lightning Climatology Studies for Idaho. Christopher D. Hill, Carl J. Gorski, and Michael C. Conger, April 1987. (PB87 180196/AS)
- 199 Heavy Rains and Flooding in Montana: A Case for Slantwise Convection. Glenn R. Lusk, April 1987. (PB87 185229/AS)
- 200 Annual Data and Verification Tabulation Eastern North Pacific Tropical Storms and Hurricanes 1986. Roger L. Cross and Kenneth B. Mielke, September 1987. (PB88 110895/AS)
- 201 An Inexpensive Solution for the Mass Distribution of Satellite Images. Glen W. Sampson and George Clark, September 1987. (PB88 114038/AS)
- 202 Annual Data and Verification Tabulation Eastern North Pacific Tropical Storms and Hurricanes 1987. Roger L. Cross and Kenneth B. Mielke, September 1988. (PB88 101935/AS)
- 203 An Investigation of the 24 September 1986 "Cold Sector" Tornado Outbreak in Northern California. John P. Monteverdi and Scott A. Braun, October 1988. (PB89 121297/AS)
- 204 Preliminary Analysis of Cloud-To-Ground Lightning in the Vicinity of the Nevada Test Site. Carven Scott, November 1988. (PB89 128649/AS)
- 205 Forecast Guidelines For Fire Weather and Forecasters - How Nighttime Humidity Affects Wildland Fuels. David W. Goens, February 1989. (PB89 162549/AS)
- 206 A Collection of Papers Related to Heavy Precipitation Forecasting. Western Region Headquarters, Scientific Services Division, August 1989. (PB89 230833/AS)
- 207 The Las Vegas McCarran International Airport Microburst of August 8, 1989. Carven A. Scott, June 1990. (PB90-240268)
- 208 Meteorological Factors Contributing to the Canyon Creek Fire Blowup, September 6 and 7, 1988. David W. Goens, June 1990. (PB90-245085)
- 209 Stratus Surge Prediction Along the Central California Coast. Peter Felsch and Woodrow Whitlatch, December 1990. (PB91-129239)
- 210 Hydrotools. Tom Egger, January 1991. (PB91-151787/AS)
- 211 A Northern Utah Soaker. Mark E. Struthwolf, February 1991. (PB91-168716)
- 212 Preliminary Analysis of the San Francisco Rainfall Record: 1849-1990. Jan Null, May 1991. (PB91-208439)
- 213 Idaho Zone Preformat, Temperature Guidance, and Verification. Mark A. Mollner, July 1991. (PB91-227405/AS)
- 214 Emergency Operational Meteorological Considerations During an Accidental Release of Hazardous Chemicals. Peter Mueller and Jerry Galt, August 1991. (PB91-235424)
- 215 WeatherTools. Tom Egger, October 1991. (PB93-184950)
- 216 Creating MOS Equations for RAWs Stations Using Digital Model Data. Dennis D. Gettman, December 1991. (PB92-131473/AS)
- 217 Forecasting Heavy Snow Events in Missoula, Montana. Mike Richmond, May 1992. (PB92-196104)
- 218 NWS Winter Weather Workshop in Portland, Oregon. Various Authors, December 1992. (PB93-146785)
- 219 A Case Study of the Operational Usefulness of the Sharp Workstation in Forecasting a Mesocyclone-Induced Cold Sector Tornado Event in California. John P. Monteverdi, March 1993. (PB93-178697)
- 220 Climate of Pendleton, Oregon. Claudia Bell, August 1993. (PB93-227536)
- 221 Utilization of the Bulk Richardson Number, Helicity and Sounding Modification in the Assessment of the Severe Convective Storms of 3 August 1992. Eric C. Evenson, September 1993.

NOAA SCIENTIFIC AND TECHNICAL PUBLICATIONS

The National Oceanic and Atmospheric Administration was established as part of the Department of Commerce on October 3, 1970. The mission responsibilities of NOAA are to assess the socioeconomic impact of natural and technological changes in the environment and to monitor and predict the state of the solid Earth, the oceans and their living resources, the atmosphere, and the space environment of the Earth.

The major components of NOAA regularly produce various types of scientific and technical information in the following kinds of publications.

PROFESSIONAL PAPERS--Important definitive research results, major techniques, and special investigations.

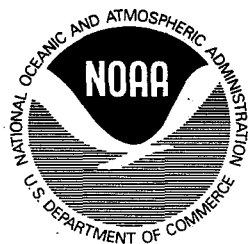
CONTRACT AND GRANT REPORTS--Reports prepared by contractors or grantees under NOAA sponsorship.

ATLAS--Presentation of analyzed data generally in the form of maps showing distribution of rainfall, chemical and physical conditions of oceans and atmosphere, distribution of fishes and marine mammals, ionospheric conditions, etc.

TECHNICAL SERVICE PUBLICATIONS--Reports containing data, observations, instructions, etc. A partial listing includes data serials; prediction and outlook periodicals; technical manuals, training papers, planning reports, and information serials; and miscellaneous technical publications.

TECHNICAL REPORTS--Journal quality with extensive details, mathematical developments, or data listings.

TECHNICAL MEMORANDUMS--Reports of preliminary, partial, or negative research or technology results, interim instructions, and the like.



Information on availability of NOAA publications can be obtained from:

NATIONAL TECHNICAL INFORMATION SERVICE

U. S. DEPARTMENT OF COMMERCE

5285 PORT ROYAL ROAD

SPRINGFIELD, VA 22161